Supplementary Information

Highly Integrated Ultra-Wide Optical and Acoustic Sensory Device: A Honeybee-Inspired Approach for Advanced Robotic Perception

Xinyu Wang[1], De Ning[1], Liguo Zhang[1], Zengxi Yang[2], Jue Gong[2*], Ting Han[1], and Xiaoran Hu[1]*

[1] School of Materials and Energy, University of Electronic Science and Technology of China, Chengdu, China

[2] Sichuan University-Pittsburgh Institute, Sichuan University, Chengdu, China

* Correspondence author: jue.gong@scupi.cn, huxiaoran@uestc.edu.cn

Environmental stability of the $FA_xMA_{1-x}PbI_3$/TFT device

After 1 Week in Ambient Air: The average photocurrent density slightly decreased to 2.4938 mA cm^{-2}, and the dark current density increased to 0.1184 mA cm^{-2}, resulting in an on/off ratio of 21.1. (Figure S1)

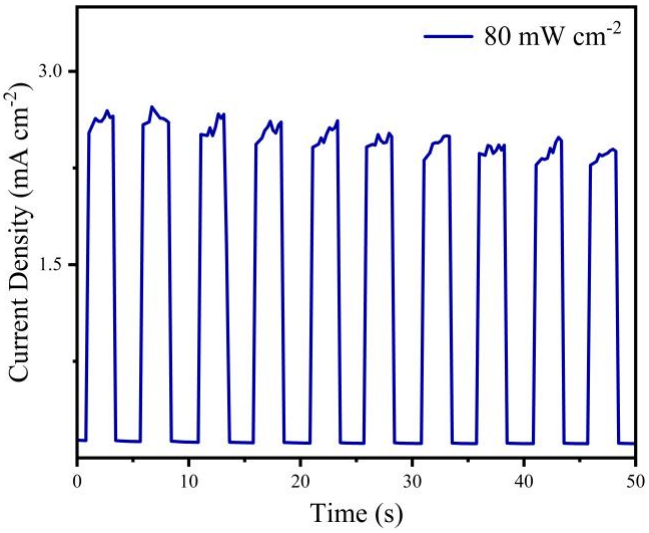

Figure S1 On-off characteristics of photonic synaptic device after one week exposure

Multidimensional spatial optical sensing reliability

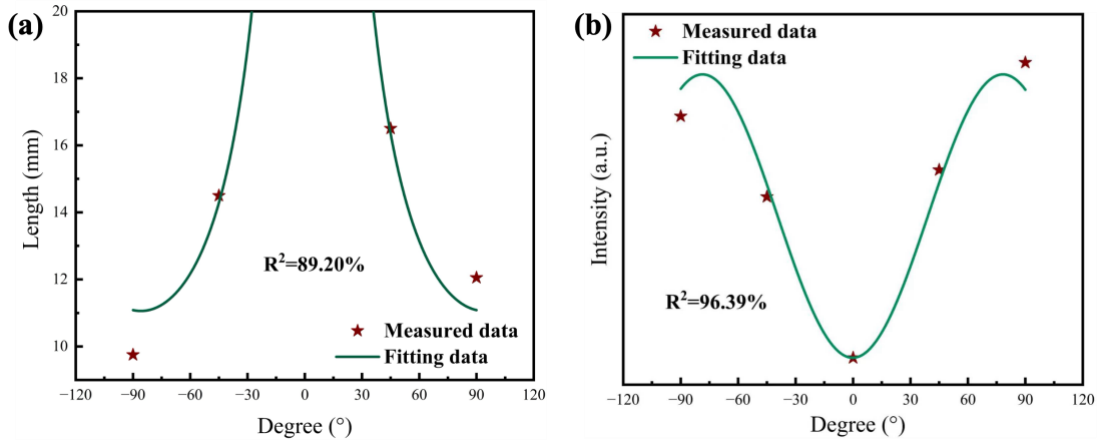

Figure S2(a) Theoretical curve fitting of the optical projection length. The red star symbols represent the experimentally extracted spot lengths from the device's line profiles at different illumination angles. The green solid line represents the theoretical geometric projection fit curve (where is $L = d/sin|\alpha|$ the diameter of the incoming light, $d = 10\,mm$), demonstrating a high correlation coefficient (R^2 = 89.20%).

Figure S2(b) Theoretical curve fitting of the peak photocurrent intensity. The red star symbols represent the experimentally extracted peak photocurrent intensities from the line profiles at various illumination angles (-90°, -45°, 0°, 45°, and 90°). The green solid line denotes the theoretical curve fit based on the radiometric cosine law, where the received irradiance (and thus the generated photocurrent) is proportional to the sine of the incident angle relative to the device surface ($I = I_0 sin|\alpha|$, where I_0 is the peak intensity read on the TFT when illuminate at 90°). The exceptionally high correlation coefficient (R^2 = 96.39%) quantitatively verifies that

the planar photonic synaptic array accurately translates angular variations in light irradiance into corresponding localized electrical responses.

Cross-talk effect

To investigate the cross-talk effect between the integrated optical and acoustic sensors on the same glass substrate, the device's optical switching behavior was recorded during simultaneous acoustic stimulation. The test was performed on the device after 1 week of environmental aging. Under the continuous acoustic vibration, the device exhibited an average photocurrent density of 2.0870 mA cm^{-2} and a dark current density of 0.4141 mA cm^{-2} (yielding a net photocurrent density of 1.6728 mA cm^{-2}). Compared to the static 1-week aged baseline, the simultaneous acoustic vibration induced only a slight baseline shift without introducing any noticeable high-frequency mechanical noise or instability into the dynamic switching cycles. The robust, clean square-wave signal confirms that the dual modalities can function independently and simultaneously with minimal cross-interference.

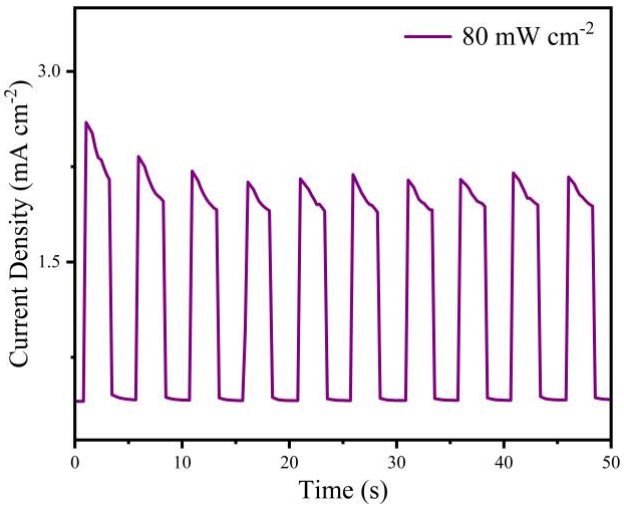

Figure S3. Dynamic photoresponse of the planar photonic synaptic device under simultaneous acoustic vibration. The device was illuminated with an 80 mW cm^{-2} light source while continuously subjected to an 80 dB, 440 Hz acoustic signal.

To further evaluate the reverse cross-modal influence from the optical modality to the acoustic modality, the output piezoelectric voltage of the PVDF-TrFE acoustic sensor was compared under dark and illuminated conditions. As shown in Figure S4, the two voltage waveforms are nearly overlapped, with comparable amplitude and temporal stability during repeated acoustic cycles. The negligible difference between the light and dark conditions indicates that optical illumination does not measurably influence the piezoelectric output or acoustic sensing performance of the PVDF-TrFE sensor.

Together with the optical response measured under acoustic vibration, these results confirm minimal cross-interference between the two integrated modalities on opposite sides of the same glass substrate.

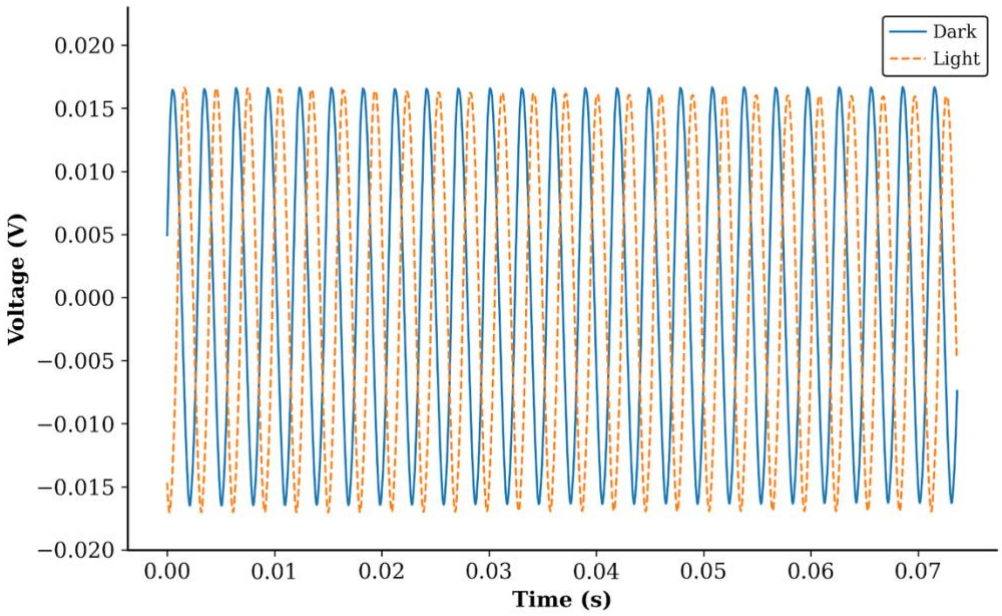

Figure S4. Output piezoelectric voltage of the PVDF-TrFE acoustic sensor measured under dark and illuminated conditions. The nearly identical voltage waveforms indicate negligible influence of optical illumination on acoustic sensing performance.

Frequency-detection accuracy of the PVDF-TrFE acoustic sensor

To quantitatively verify the effectiveness of the acoustic detector in resolving frequency information from different sound sources, the frequency-detection accuracy of the PVDF-TrFE acoustic sensor was evaluated using programmed sound signals from 1 to 12 kHz. The output piezoelectric voltage signals were recorded, and the detected frequencies were extracted and compared with the programmed input frequencies. As shown in Figure S5, the detected frequency displays an excellent linear relationship with the input frequency, with a fitting equation of $y = 0.9997x + 0.0021$ and a high coefficient of determination ($R^2 = 0.999984$). Across the entire measurement range, the average absolute error is 9.3 Hz, and the maximum relative deviation remains within 0.33%. These results demonstrate that the PVDF-TrFE acoustic sensor can accurately convert acoustic frequency inputs into corresponding electrical signals, supporting the validity and effectiveness of distinguishing different acoustic sources.

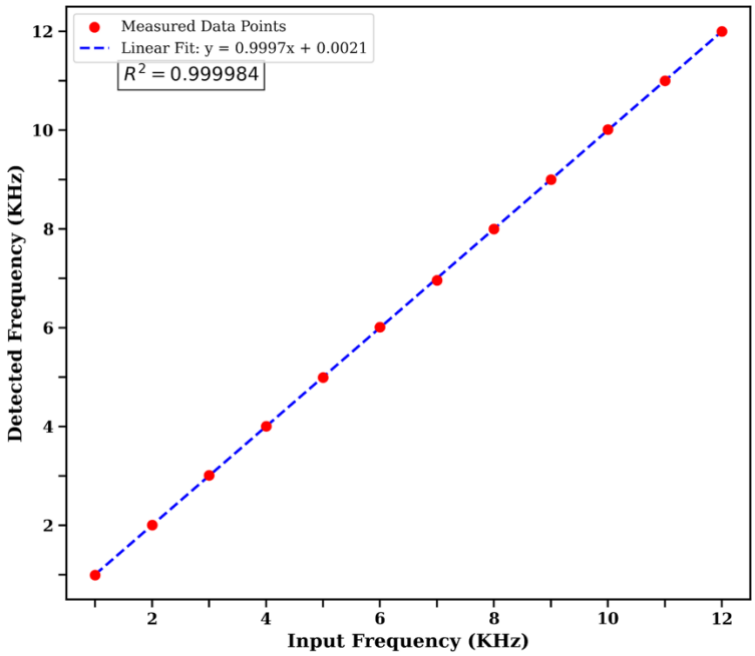

Figure S5. Frequency-detection accuracy of the PVDF-TrFE acoustic sensor under acoustic stimuli from 1 to 12 kHz. The red symbols represent the measured detected frequencies extracted from the piezoelectric voltage response, and the blue dashed line represents the linear fitting result.

Fatigue/cyclic stability of the PVDF-TrFE acoustic sensor

To evaluate the fatigue/cyclic stability of the PVDF-TrFE acoustic sensor, the device was continuously stimulated by a 328 Hz acoustic signal. A total of 10,000 output-voltage data points, corresponding to 131 consecutive cycles, were recorded. As shown in Figure S6, the piezoelectric voltage waveform maintains highly consistent amplitude and periodic shape throughout the test, without obvious attenuation, distortion, or baseline drift. This result demonstrates the excellent anti-fatigue performance and stable repeated acoustic response of the PVDF-TrFE sensor.

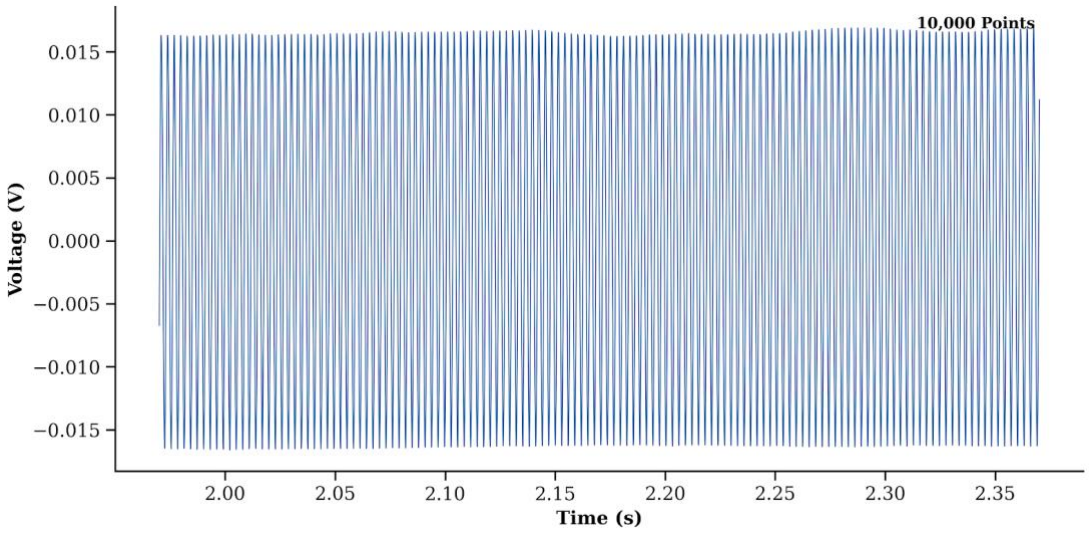

Figure S6. Fatigue/cyclic stability test of the PVDF-TrFE acoustic sensor under a 328 Hz acoustic signal. The output waveform contains 10,000 data points across 131 consecutive cycles, showing a highly consistent voltage response.